JOURNAL OF GEOPHYSICAL RESEARCH, VOL. 103, NO. D12, PAGES 13,713–13,728, JUNE 27, 1998

Moisture budget in the tropics and the Walker circulation

V. Brahmananda Rao, S. R. Chapa, and I. F. A. Cavalcanti
Instituto Nacional de Pesquisas Espaciais (INPE), São José dos Campos, São Paulo, Brazil

Abstract. Moisture budget in the tropics is studied for two contrasting years, 1987 (El Niño) and 1988 (La Niña), and for two seasons, December, January, and February (DJF) and June, July, and August (JJA). To evaluate the moisture budget, data from the National Centers for Environmental Prediction (NCEP) reanalysis are used. First, the mean rainfall and evaporation characteristics of the NCEP reanalysis for January, April, July, and October are compared with other independent data. The general precipitation zones associated with the large-scale features such as Intertropical Convergence Zone (ITCZ), South Pacific Convergence Zone (SPCZ), and South Atlantic Convergence Zone (SACZ) seem to be captured by the NCEP reanalysis. However, the seasonal variations, as seen in other data, are not reproduced well. Characteristics of ITCZ in the eastern Pacific is not well reproduced in the NCEP reanalysis data. The overall characteristics of latent heat flux (evaporation) in the NCEP reanalysis seem to be in qualitative agreement with other independent data. However, there are quantitative differences. The differences in rainfall over the western Pacific between DJF 1986/1987 (El Niño) and DJF 1988/1989 (La Niña) are associated with the differences in the position and intensity of SPCZ. The SPCZ is more intense in the El Niño year and is displaced northeastward. Northeast Brazil experienced higher rainfall in DJF 1988/1989 than in DJF 1986/1987. During the boreal summer (monsoon) season (JJA), rainfall was higher in 1988 over India than in 1987. The NCEP rainfall data are compared with the rainfall data from Schemm et al. and Huffman et al. The NCEP reanalysis seems to underestimate rainfall over the equatorial eastern Pacific. Higher precipitable water is found over the regions of intense convection such as SACZ, SPCZ, ITCZ, and the monsoon trough in JJA. The NCEP reanalysis seems to capture the general characteristics of vertically integrated moisture transport such as the general westward transport in the tropics, cross-equatorial moisture transport over the Indian Ocean with high values near the Somali coast in JJA. Over the western Pacific the differences between the two periods are associated with differences in moisture convergence but not evaporation. The increment term (D_c) shows large values over the mountainous regions. The evaluation of moisture budget of the Walker circulation shows that over the western Pacific the large differences in precipitation between the two contrasting years are accounted mainly by the differences in moisture flux convergence. This verifies the important role of moisture convergence in this region as inferred indirectly by Cornejo-Garrido and Stone. However, over the Amazon region, evapotranspiration seems to play an important role in the local precipitation.

1. Introduction

Moisture plays a key role in several aspects of human life such as water supply for daily needs and agriculture. Yet the global hydrological cycle is poorly understood, and only recently, attempts are being made to study the causes of long-term widespread droughts and floods. Before 1980 the operational analyses did not permit a realistic evaluation of the hydrological cycle [*Rosen and Salstein*, 1980]. *Trenberth* [1991] studied the moisture budget from the ECMWF (European Centre for Medium-Range Weather Forecasts) data and obtained realistic patterns. *Trenberth and Guillemot* [1995] evaluated and compared the hydrological cycle in the NMC (National Meteorological Centre) and ECMWF analyses and noted relative differences. *Rasmusson and Mo* [1996] found that the hydrological cycle derived from the NCEP (National Centers for Environmental Prediction) operational products were useful descriptions of the atmospheric branch of the hydrologic cycle. *Mo and Higgins* [1996] compared the general features of the hydrological cycle in the NCEP/NCAR (National Center for Atmospheric Research) and NASA Data Assimilation Office (DAO) reanalysis products. They concluded that the NCEP reanalysis can be used to examine broad aspects of the atmospheric hydrological cycle.

One source of interannual variability in floods and droughts is the El Niño Southern Oscillation (ENSO) phenomenon, which is responsible for the extreme phases of opposite sign in rainfall in the tropics and subtropics [*Glantz et al.*, 1991]. Two extreme climatic events occurred in 1987 and 1988 and were associated with the 1986–1989 ENSO cycle. The 3 year period (1986–1989) spans a complete ENSO cycle during which sea surface temperature (SST) in the central and the equatorial Pacific evolved through a moderate warming and a strong cooling cycle. The 1988 La Niña event is the strongest in the last 20 or more years [*Trenberth and Guillemot*, 1996]. Two extreme events, one drought and the other flood occurred over India in the summer monsoon seasons of 1987 and 1988. All

Paper number 98JD00943.
0148-0227/98/98JD-00943$09.00

India "average" rainfall during June, July, August, and September (JJAS) was nearly two standard deviations below and above normal in 1987 and 1988, respectively [*Krishnamurti et al.*, 1989, 1990]. Other regions in the tropics were also affected. Several parts of South America experienced opposite rainfall anomalies with less rainfall in 1987 and higher rainfall in 1988 [*Rao and Lima*, 1995]. Over North Africa, rainfall was well below normal in JJA 1987 and almost normal in 1988 [see *Rowell et al.*, 1995, Figure 3; *Ba et al.*, 1995, Figure 12]. So far, characteristics of the moisture budget for the 1986–1989 ENSO cycle have not been discussed in detail except for a brief discussion by *Mo and Higgins* [1996]. The purpose of the present study is to evaluate the moisture budget in the tropics for the 1986–1989 ENSO cycle. We use the NCEP reanalysis data for this purpose. We try to identify limitations and merits of these data by comparing with other independent data wherever possible.

One important aspect of the general circulation in the tropics is the so-called Walker circulation. The circulation in the equatorial plane with rising motion in the western Pacific and sinking motion in the eastern Pacific was called by *Bjerknes* [1969] as the Walker circulation. There is considerable interannual variability in the scale and intensity of the Walker circulation. This variability is related to ENSO. Although *Bjerknes* [1969] concentrated on the circulation in the Pacific Ocean, a more satisfactory formal definition is that due to *Newell et al.* [1974]. They defined the Walker circulation as the circulation in the equatorial vertical plane covering all the longitudes [see *Newell et al.*, 1974, Figure 9.3]. One notes several cells of rising and sinking motion in this picture of the Walker circulation. These rising and sinking cells are associated with high or low rainfall, and the interannual variability in the positions of the rising and sinking limbs of the Walker circulation is associated with the interannual variation of rainfall.

Regarding the generation of the Walker circulation, *Bjerknes* [1969] suggested that it is driven by the gradient of SST along and south of the equator in the Pacific. He conjectured that over the eastern Pacific the air above the cold water belt cannot join the ascending motion in the Hadley circulation. Instead, the equatorial air flows westward to the western Pacific where it is supplied with moisture and heat from relatively warm water and can therefore take part in the large-scale moist adiabatic ascent. An underlying assumption in this picture of the Walker circulation is that the source of the precipitation, which drives the circulation, is the local evaporation associated with warm SST. However, the heat balance study by *Cornejo-Garrido and Stone* [1977] suggests that the primary drive for the Walker circulation is the longitudinal variation of condensation. They also noted that in the regions where the condensation is maximum, the evaporation is minimum. Nevertheless, the Bjerknes hypothesis might still be invoked as an initiating mechanism for the Walker circulation.

The results of *Cornejo-Garrido and Stone* [1977] implies that the excess of condensation heating in the region of maximum condensation is supplied by the horizontal convergence of moisture. Thus the second objective of the present study is to verify whether this is in fact the case or not with an actual calculation of the moisture budget of the Walker circulation. We study the moisture budget of the Walker circulation for the 1986–1989 ENSO cycle giving emphasis to the DJF (December, February, and January) season. We will try to estimate the relative roles of evaporation and moisture convergence (or divergence) in the interannual variation of precipitation associated with the Walker circulation.

2. Data Sources and Methodology

The data used in this study are monthly means of zonal wind (u), meridional wind (v), specific humidity (q), precipitable water (W), and precipitation (P) of the NCEP/NCAR reanalysis for 1986–1989 period. Data have a horizontal resolution of 2.5° × 2.5° (latitude and longitude) and span globally. Data at 1000, 925, 850, 700, 600, 500, 400, and 300 hPa are used in this study. Detailed description of the assimilation systems and output are given by *Kalnay et al.* [1996]. In this study we compare the rainfall climatologies from the NCEP reanalysis with the rainfall from the Microwave Sounding Unit (MSU) over oceans and station observations [*Schemm et al.*, 1992]. *Mo and Higgins* [1996] made a comparison of these data for the annual mean rainfall and analyzed the realistic differences and agreements. Since we propose to study seasonal variation, here we compare the long-term means for January, April, July, and October. We also use Global Precipitation Climatology Project (GPCP) results of *Huffman et al.* [1997]. As noted by *Mo and Higgins* [1996], the validation is not absolute. There are uncertainties in the observations as well.

The moisture budget equation can be written as

$$\frac{\partial W}{\partial t} = -D(Q) + E - P \tag{1}$$

where $D(Q) = \nabla \cdot Q$

$$Q = \frac{1}{g}\int_{p_t}^{p_0} \overline{qV}\, dp \tag{2}$$

where p_t = 300 hPa, p_0 = 1000 hPa, g is the acceleration of gravity, and V is the vector wind. Equation (1) states that the change of the total precipitable water in the column W is equal to the difference between evaporation (E) and the sum of precipitation (P) and the vertically integrated moisture flux divergence $D(Q)$. For long-term means, $(\partial W/\partial t)$ is small, and so (1) becomes

$$E - P = D(Q) \tag{3}$$

Equation (3) is valid for observations and numerical model simulations. When the fields Q, E, and P are produced with a data assimilation system, the correct budget equation is given by [*Schubert et al.*, 1995],

$$\nabla \cdot Q = E - P + D_c \tag{4}$$

where D_c represents the increment of the model state by the observational data. A simple way of estimating D_c is by using

$$D_c = \nabla \cdot Q - E + P \tag{5}$$

It should be noted here that since monthly means are used, the water vapor flux by transient eddies is not included in (2). However, as shown by several authors [*Chen*, 1985; *Rao et al.*, 1996], the contribution by transient eddies for the total water vapor flux is less than 10% in the tropics. Also, we propose to calculate the moisture budget on pressure surfaces which is different from the model grid. In addition, we have no moisture data above 300 hPa. Thus D_c includes all these increments. The discussion of possible errors in the calculation of the divergence of moisture flux is given by *Rao et al.* [1996].

3. Mean Rainfall and Evaporation

In this section we compare mean (1982–1994) rainfall and evaporation from the NCEP reanalysis with other independent data. Figures 1a–1d show the NCEP mean rainfall for January, April, July, and October. Figures 2a–2d show mean (1979–1992) rainfall for these four months from *Schemm et al.* [1992]. We also compare Figure 1 with Figure 4 of *Huffman et al.* [1997], which is for the four seasons of 3 months period each.

The precipitation zones associated with the large-scale characteristics seem to be captured by the NCEP reanalysis. The southeastern Asian monsoon is evident in Figure 1 with maximum intensity in July. Oceanic rainfall maxima to the east and west of India can be seen in Figure 1c. Similar features are seen in our Figure 2 and Figure 4 of *Huffman et al.* [1997]. The rainfall patterns in the Indian Ocean in Figure 1c are very similar to those seen in Figure 4 of *Huffman et al.* [1997] for the season June, July, and August (JJA). The patterns in Figure 2c in this region are different. The monsoon precipitation maximum shifts east and southward in October (Figure 1d). A similar feature is seen in Figure 4 of *Huffman et al.* [1997] for the season September, October, and November (SON). Although a similar feature is seen in Figure 2d, the pattern is a little different. The south and eastward shift of rainfall reaches northern Australia in January. This is seen in the other two figures also.

In the Pacific the precipitation zones associated with the ITCZ (Intertropical Convergence Zone) and the SPCZ (South Pacific Convergence Zone) are seen in Figure 1a. However, the seasonal variation of these two features, as seen by *Schemm et al.* [1992] and *Huffman et al.* [1997], is not reproduced well by the NCEP reanalysis. Particularly the ITCZ in the eastern Pacific is less intense in the NCEP reanalysis in July and October. In the works of *Huffman et al.* [1997] and *Schemm et al.* [1992] the northwest to southeast orientation of the SPCZ is very clear in all the months. Similar orientation is not clearly seen in the NCEP reanalysis.

The principal feature in the austral summer season over South America is the South Atlantic Convergence Zone (SACZ) with a northwest to southeast orientation. This feature is very clearly seen by *Schemm et al.* [1992] and *Huffman et al.* [1997] data. In the NCEP reanalysis, although there is a similar feature, its extension into the Atlantic Ocean is limited. Also, the ITCZ in the equatorial Atlantic of NCEP fields is not so sharp as in the other two figures. As noted earlier, the ITCZ in the eastern Pacific is also not reproduced well in the NCEP fields, thus suggesting a problem in detail reproduction of the ITCZ in the NCEP reanalysis. *Mo and Higgins* [1996] also noted similar problems in the annual mean rainfall. However, the differences seem to increase in individual seasons. It should be noted that the estimates of precipitation from microwave measurements over the oceans by *Schemm et al.* [1992] are redone and are observed to be lowered by 20%. However, credence should be given to the differences in the patterns rather than to the magnitudes. Estimates of D_c are given in section 4.

Next, we compare the latent heat flux (evaporation) in the NCEP reanalysis for January, April, July, and October (Figure 3) with other independent data. Most of the earlier estimates of evaporation [*Hsiung*, 1986; *Cayan*, 1992] were based on the use of aerodynamic bulk formulae. The main problem with this method is the choice of values for the transfer coefficients which vary with the wind speed and the stability of the atmosphere [*Smith*, 1988]. Further, these estimates do not include important bias corrections of the observations [*Da Silva et al.*, 1994; *World Climate Research Program* (*WCRP*), 1996]. *Da Silva et al.* [1994] carefully analyzed fluxes from Comprehensive Ocean-Atmospheric Data Set (COADS) data and found that it is necessary to empirically increase the evaporation by 16% to achieve a reasonable surface energy balance. *Oberhuber* [1988] made a similar correction to his evaporation estimation.

In a recent study, *Jourdan and Gautier* [1995] compared latent heat flux derived from Special Sensor Microwave/Imager (SSM/I) sensor data with that from the COADS. *Jourdan and Gautier* [1995] adopted a method to estimate evaporation which is based on the similarity theory [*Businger*, 1975; *Liu et al.*, 1979]. Statistical relations have been used to derive relevant parameters from satellite precipitable water fields, and both satellite-derived and in situ parameters have been put into a model that is based on similarity theory to compute evaporation. A similar procedure is used to obtain evaporation from the COADS data. In an attempt to improve the global evaporation estimate, *Jourdan and Gautier* [1995] developed a ship-satellite blending procedure. A comparison between the blended and the COADS evaporation shows much improvement in the regions previously identified as having large and systematic differences. Their results are only for January and July. Their Figures 6 and 7 can be compared with our Figures 3a and 3c. The qualitative agreement between the maps is good in the sense that similar features are found at the same location both in January and in July. The high evaporation in the western oceans in January is similar in both data sets. The high evaporation over the South Indian Ocean, Arabian Sea, and Bay of Bengal in July is also similar. Low values of evaporation are found in the low-level convergence zones, especially in the eastern Pacific and Atlantic Oceans in both data sets. However, there are quantitative differences. Satellite values seem to overestimate evaporation in high-evaporating regions particularly in the southeastern Pacific both in January and July compared to the NCEP reanalysis and the COADS data. In the regions of low evaporation, satellite values are underestimated. The region where this happens is in January between 0° and 10°S in the eastern Atlantic. The blended latent heat flux is found to agree within 28 W m^{-2} with the COADS computations when the in situ sampling is good enough. Significant improvements are observed in the blended analysis [*Jourdan and Gautier*, 1995, Figure 17] over the eastern part of the three basins. Changes are also observed in the southeastern Pacific along the coast of South America where evaporation values are comparable both in the NCEP reanalysis and in the blended analysis of *Jourdan and Gautier* [1995].

4. Moisture Budget in the Tropics for Two Contrasting Years

Figures 4a, 4b, and 4c show the rainfall for DJF 1986/1987, DJF 1988/1989, and their difference, respectively. Higher rainfall over the subtropics of the southwestern Pacific is clearly seen during the El Niño period 1986/1987 compared to the La Niña period 1988/1989. Thus positive anomalies are seen over this region in Figure 4c. These anomalies are associated with the changes in the position of the SPCZ. The rainfall in the equatorial Pacific is associated with the ITCZ. The mean positions of these two systems are given in Figure 1 of *Vincent* [1994]. As noted by Vincent, the SPCZ seems to be more intense and moves northeastward during an El Niño year com-

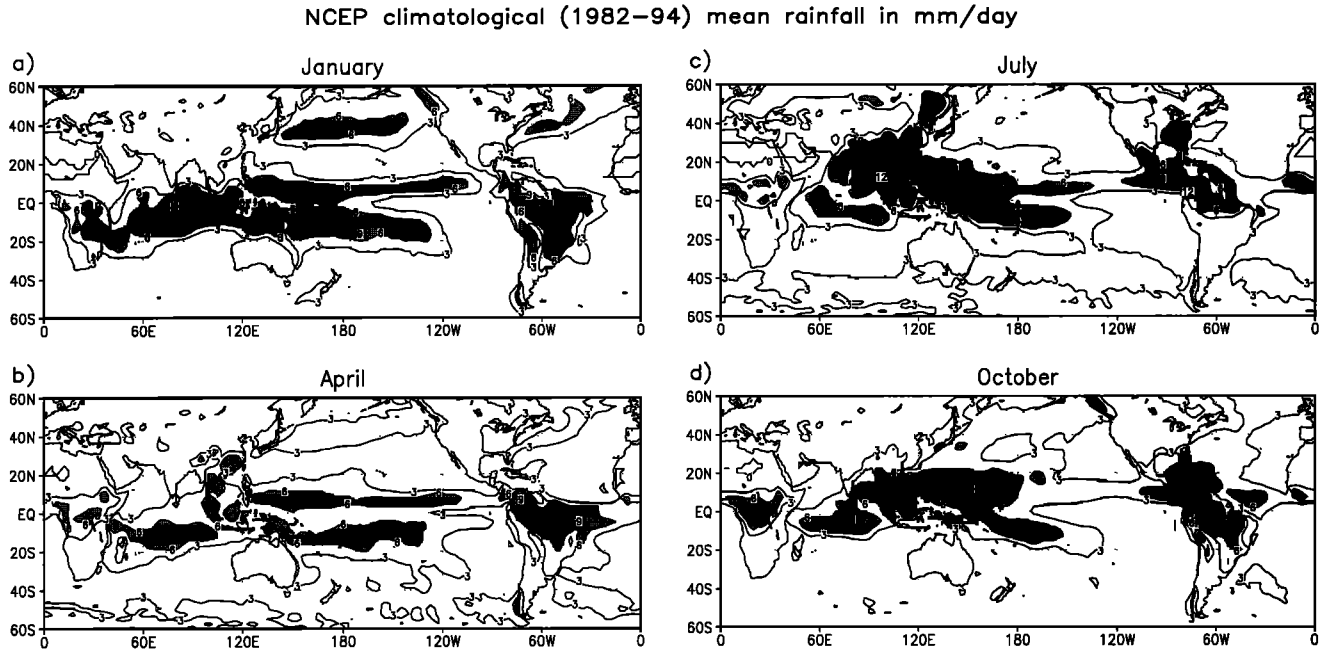

Figure 1. Mean (1982–1994) rainfall in mm/d for (a) January, (b) April, (c) July, and (d) October from NCEP reanalysis.

pared to the mean position. Somewhat higher rainfall is observed in DJF 1988/1989 over northern South America, in particular over northeastern Brazil, showing generally negative values in Figure 4c over this region. Negative values are also seen over the Carribean Sea and positive values to the north of it.

Figures 4d, 4e, and 4f show the rainfall for JAS 1987, JAS 1988, and the difference between them, respectively. As expected, rainfall is high over the equatorial Indian Ocean, India, eastern Asia, and central Africa. Rainfall is high over the Mexican monsoon region also. In Figure 4f, positive anomalies are seen over the equatorial central Pacific, showing that the rainfall was higher during the El Niño year over this region. Negative anomalies are seen over India and equatorial Indian Ocean indicating higher rainfall in the La Niña year JJA 1988 than in the El Niño year JJA 1987. Negative values are also seen over Central Africa.

Huffman et al. [1997] analyzed the differences in rainfall from satellite/gauge (SD) estimate for the El Niño and La Niña episodes (their Figure 8). The top panel of their Figure 8 shows the differences for the DJF season for the warm episode of DJF 1991/1992 and a cold episode of DJF 1988/1989. Although this figure is for a different period, the differences in rainfall between the El Niño and the La Niña episodes can be compared with our Figure 4c. The patterns in precipitation are very similar. Positive values in the central Pacific and the eastern Pacific ITCZ and negative values to the west are very similar in

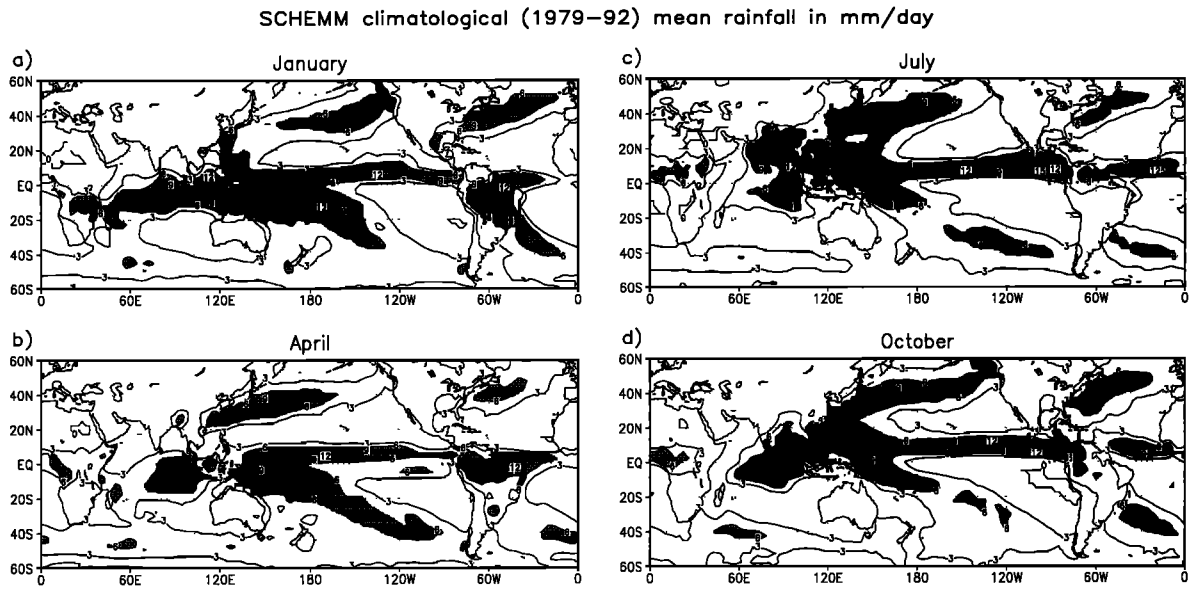

Figure 2. Same as Figure 1 but from *Schemm et al.* [1992].

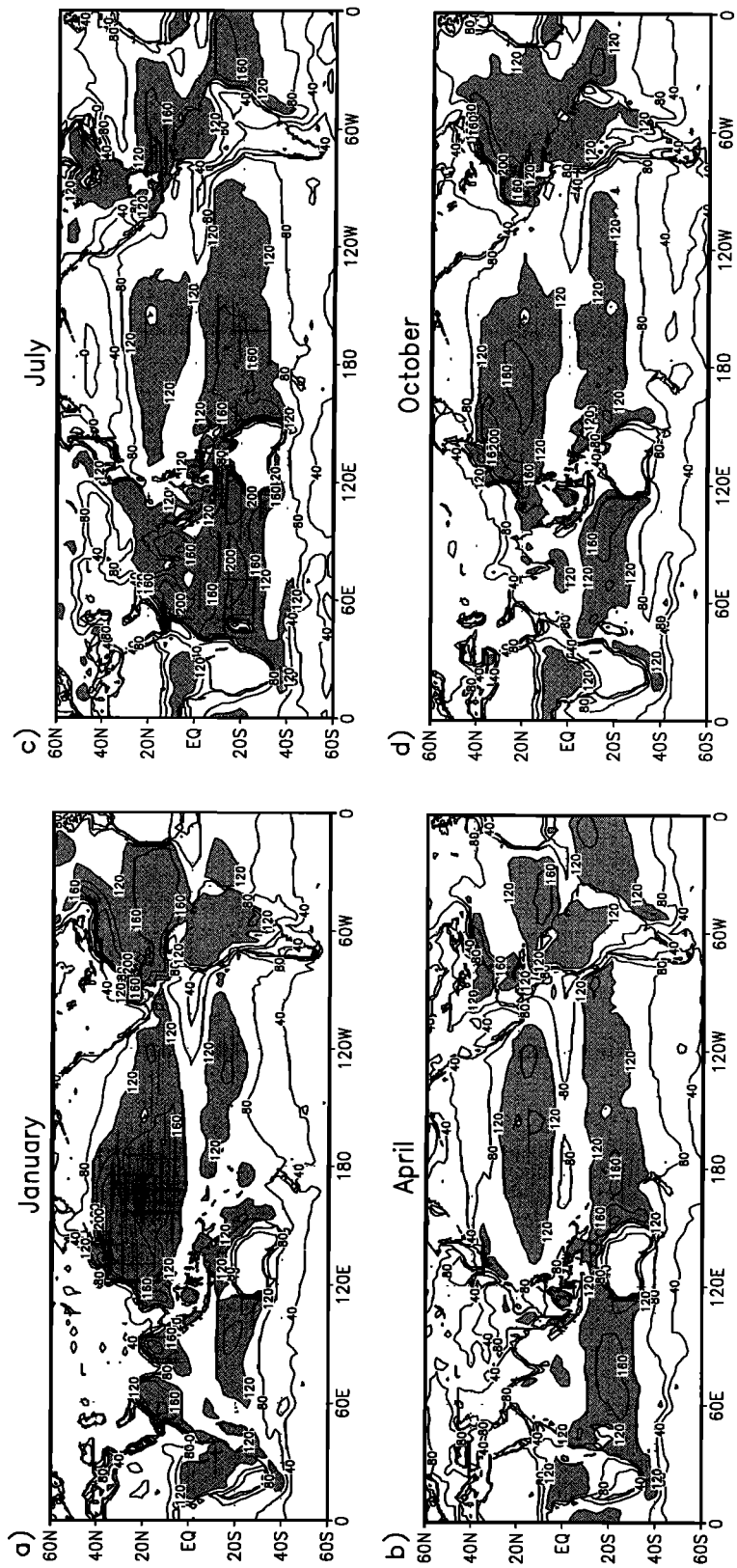

Figure 3. Mean (1982–1994) vertical latent heat flux (evaporation) in W/m^2 for (a) January, (b) April, (c) July, and (d) October.

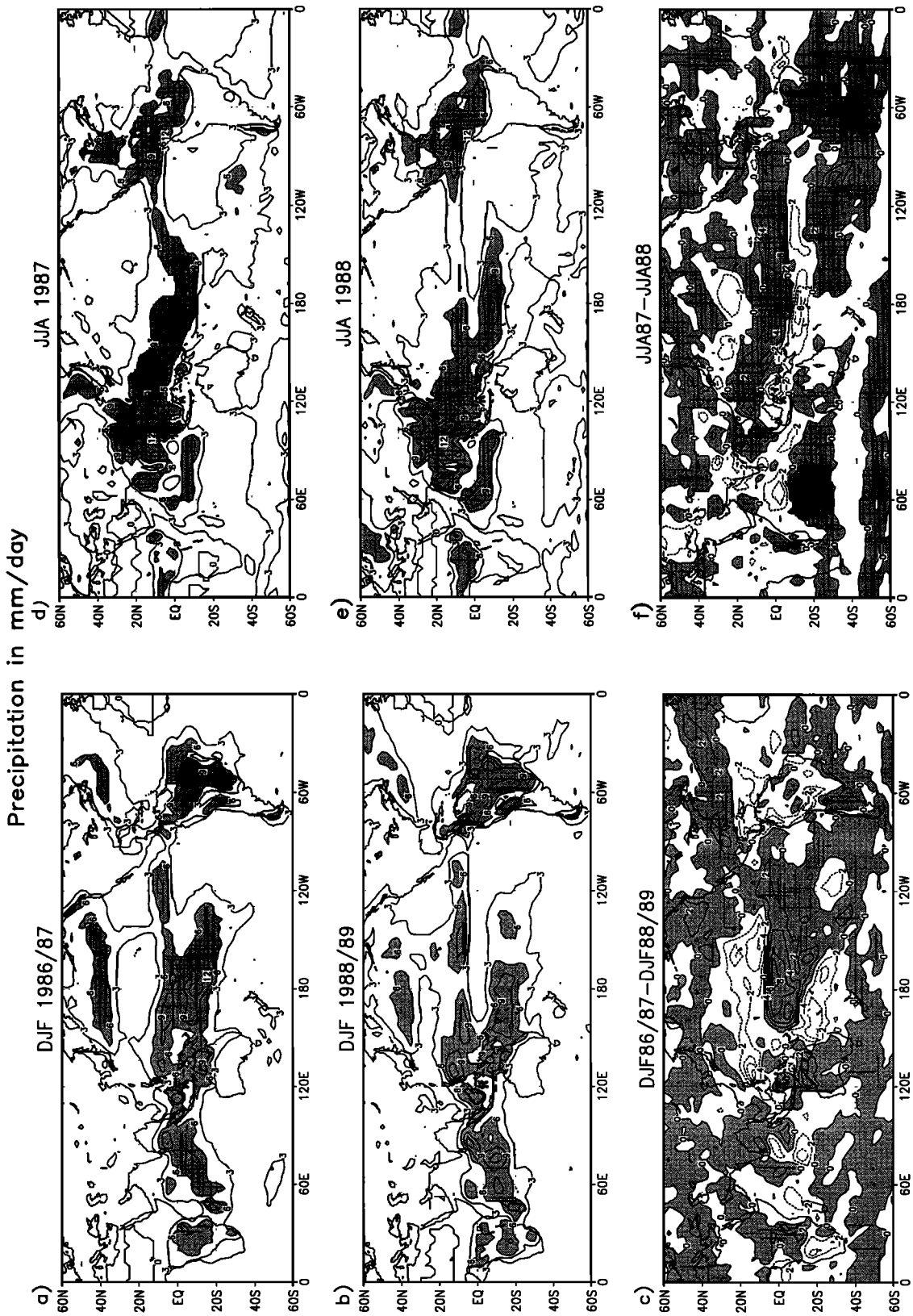

Figure 4. Precipitation in mm/d for (a) DJF 1986/1987, (b) DJF 1988/1989, (c) the difference between them, (d) JJA 1987, (e) JJA 1988, and (f) the difference between them.

both figures. The differences over South America are also similar.

The bottom panel of Figure 8 of *Huffman et al.* [1997] can be compared with our Figure 4f. Both figures are for the JJA season of the same El Niño (1987) and La Niña (1988) episodes. A band of positive values along the equator is similar in both figures. Negative values over India and the equatorial Indian Ocean are also similar. Thus the NCEP reanalysis seems to capture the differences in rainfall between the El Niño and the La Niña episodes.

Figure 5 shows precipitable water (mm) during the El Niño and La Niña years for the austral summer and winter seasons. High precipitable water is expected in the regions of intense convection such as the SACZ, SPCZ, ITCZ, and the monsoon trough in JJA which is indeed the case. More precipitable water is seen over the oceans than over the continents. Precipitable water generally increases from the eastern Pacific Ocean to the western Pacific Ocean showing a close connection with the SST. A comparison of Figures 4c and 5c shows that higher precipitation over the central Pacific during the El Niño year in DJF 1986/1987 was associated with higher precipitable water. A similar feature is also observed in the austral winter season (Figures 4f and 5f). In both seasons, in this area, the precipitable water changes are larger than the precipitation changes. Over the Indian subcontinent, the high precipitation in JJA 1988 was associated with higher precipitabe water. A close examination of Figures 4c and 5c shows that over northeastern Brazil, higher precipitation in DJF 1988/1989 was not associated with higher precipitable water. A similar feature was noted earlier by *Rao and Marques* [1984].

Figure 6 shows the vertically integrated water vapor transport for austral summer and winter seasons for the two contrasting years. In Figures 6a and 6b, during the austral summer season, the water vapor transport is mainly westward in the tropics because of trade winds. Anticyclonic cells of water vapor transport are evident in both the Atlantic and the Pacific. The important role of the tropical Atlantic in supplying water vapor to the Amazon Basin can be noted. These are some of the features noted by earlier authors [*Chen*, 1985; *Rao et al.*, 1996]. In Figure 6c, anticyclonic cells of water vapor flux can be noted on either side of the equator in the western Pacific. In this region, strong eastward transport is seen along the equator.

During the boreal summer (Figures 6d, 6e, and 6f) the water vapor transport due to the monsoon flow is clearly seen over the Indian Ocean, Arabian Sea, and Bay of Bengal in both years. The water vapor transport by the monsoon flow was more in JJA 1988 than in JJA 1987, such that the difference between them shows outward transport from the Indian peninsula and eastward transport over the Indian Ocean (Figure 6f). In both years the transport of water vapor from the South Indian Ocean across the equator was small over the longitudes 60°–90°E. Large values of cross-equatorial transport are noted near the Somali coast, probably associated with the Somali current. The importance of low-level monsoon circulation for supplying moisture for the monsoon rainfall over India has been noted by *Murakami et al.* [1984] and *Chen and Van Loon* [1987]. Over eastern Asia the transport of moisture is westward across the Pacific. An anticyclonic cell of moisture flux over the subtropical western Pacific can be seen in Figure 6f. A similar feature can be noted in Figure 9a of *Mo and Higgins* [1996].

Figure 7 shows the divergence of moisture flux ($\nabla \cdot Q$) in mm/d for the austral summer and winter seasons. A comparison of Figures 4a, 4b, 4c, and 7a, 7b, 7c shows that regions of high precipitation are in general associated with convergence of moisture flux. Such regions are the western equatorial Pacific, continental South America, and the southern Indian Ocean. The magnitudes also agree approximately. Regions of low precipitation are associated with divergence of the moisture flux. A comparison of Figures 4c and 7c shows that the region of higher precipitation during the El Niño year in the western Pacific was associated with higher convergence (negative values), and the magnitudes are also similar. To the north and south of this region, low precipitation during the El Niño years was associated with higher divergence (positive values in Figure 7c). This shows that in these places the differences in rainfall during the two contrasting years was associated with the changes in convergence of water vapor flux but not due to the changes in evaporation. As we shall see later, the evaporation changes are much less in magnitude. This supports the conclusions of *Deser and Wallace* [1990], *Ramage and Hori* [1981], and *Mo and Higgins* [1996]. However, over the Amazon Basin, evaporation seems to have a major role [*Salati and Nobre*, 1991]. This will be discussed in a later section while evaluating the moisture budget of the Walker circulation.

Figures 7d, 7e, and 7f show the divergence of moisture flux for the boreal summer seasons of 1987 and 1988 and their difference, respectively. Again, there is a general agreement between the high rainfall regions (Figures 4d, 4e, and 4f) and the moisture flux convergence. A comparison of Figures 4f and 7f shows that over the equatorial western Pacific the higher precipitation in JAS 1987 coincides with the region of higher convergence. Over India, also a similar agreement is seen.

Figure 8 shows the evaporation (mm/d) for DJF 1986/1987 and DJF 1988/1989 and JJA 1987 and JJA 1988. Some of the general features of the evaporation in these figures are similar to the characteristics of the mean evaporation noted earlier (Figure 3). One interesting feature noted in Figures 8a, 8b, and Figures 4a, 4b is that the regions of high evaporation over the western oceans are not associated with high rainfall. This shows that the moisture gained by the atmosphere in these regions from the ocean is carried away to other regions. In Figures 8d, 8e, and 4d, 4e it can also be seen that the high evaporation over the southern Indian Ocean, Arabian Sea, and Bay of Bengal is fed into the precipitating monsoon regions (see also Figure 6d and 6e). It can be seen in Figures 8c and 8f that the evaporation changes are much less than the rainfall changes. As has already been noted, this suggests that the interannual variations of rainfall is accounted essentially by the interannual variations of moisture convergence.

Figure 9 shows the analysis increment term D_c, calculated from (5). Large values are noted over mountainous regions to the north of India and over Andes. D_c is large over other regions, such as northern Africa and central America and also over the eastern coast of South America.

5. Moisture Budget of the Walker Circulation

In this section we will discuss the moisture budget of the Walker circulation for two contrasting years. Figure 10 shows the rainfall (mm/d) from the NCEP reanalysis at three latitudes 0°, 5°S, and 10°S for the two contrasting periods DJF 1986/1987 (continuous line) and DJF 1988/1989 (broken line). Since the Walker circulation is not confined to the equator, three latitudes are chosen for the present discussion.

At the equator and 5°S, large changes in rainfall between El Niño and La Niña years are seen over the southwestern Pacific

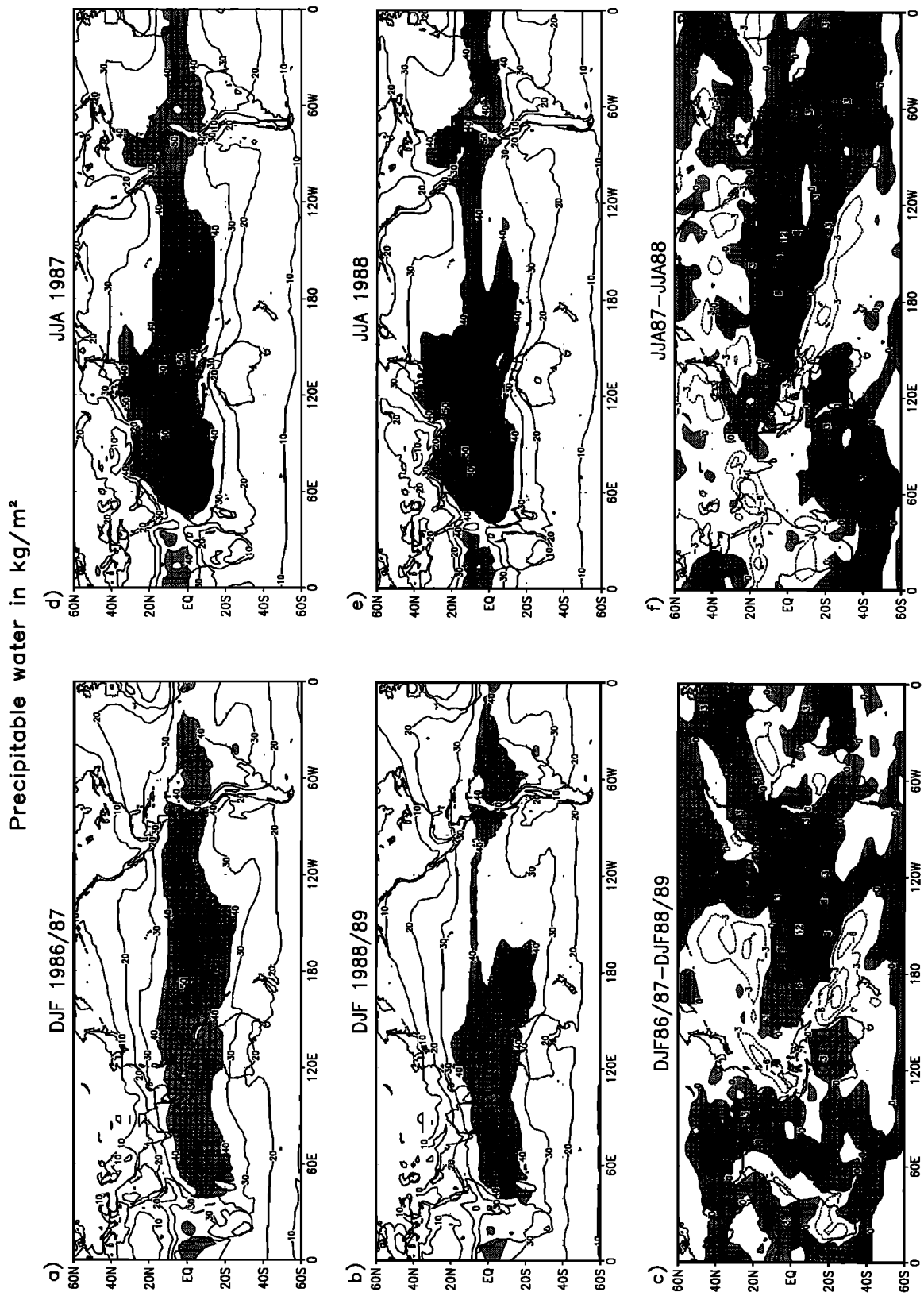

Figure 5. Precipitable water in kg/m^2 (mm) for (a) DJF 1986/1987, (b) DJF 1988/1989, (c) the difference between them, (d) JJA 1987, (e) JJA 1988, and (f) the difference between them.

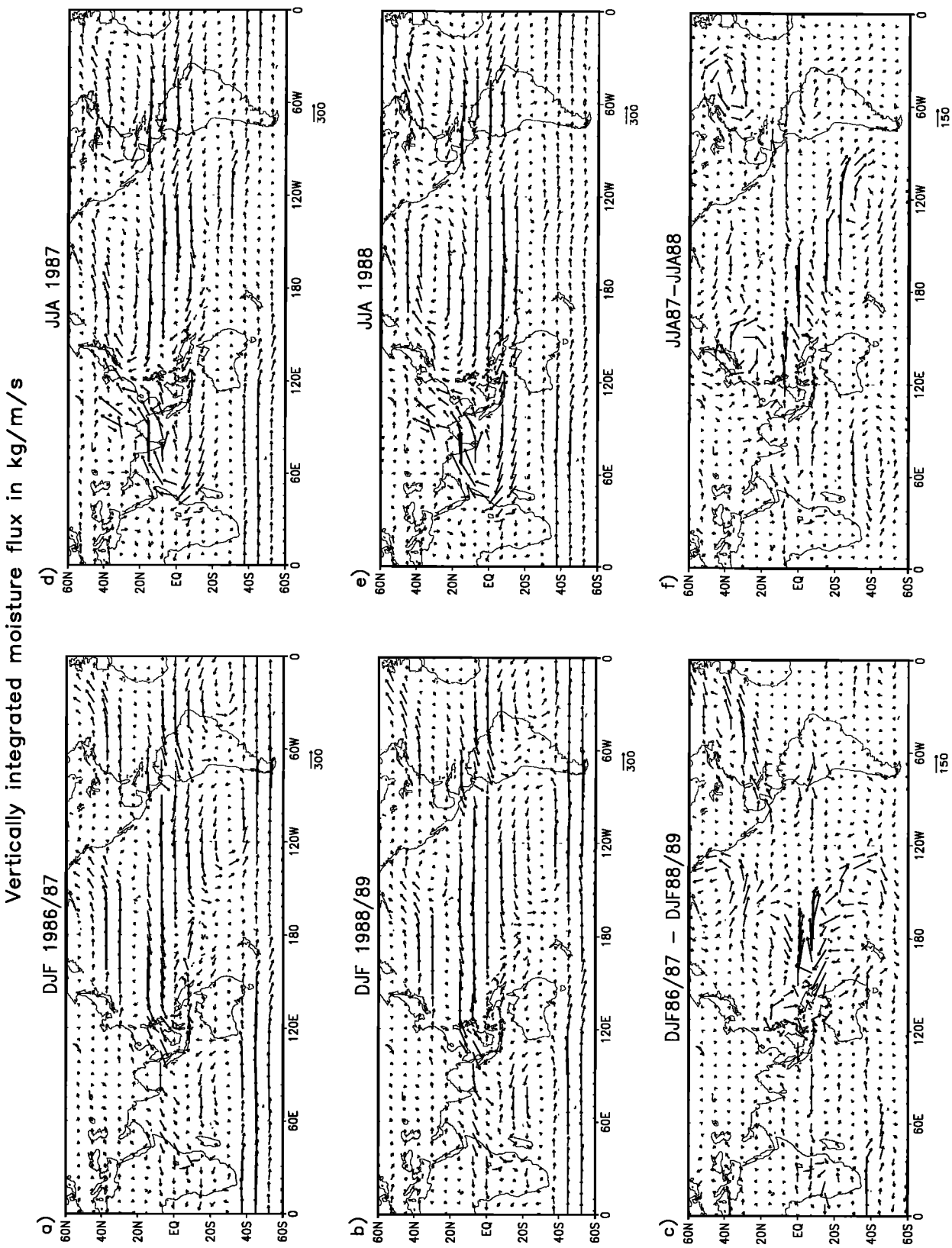

Figure 6. Vertically integrated moisture transport (kg/m/s) for (a) DJF 1986/1987, (b) DJF 1988/1989, (c) the difference between them, (d) JJA 1987, (e) JJA 1988, and (f) the difference between them.

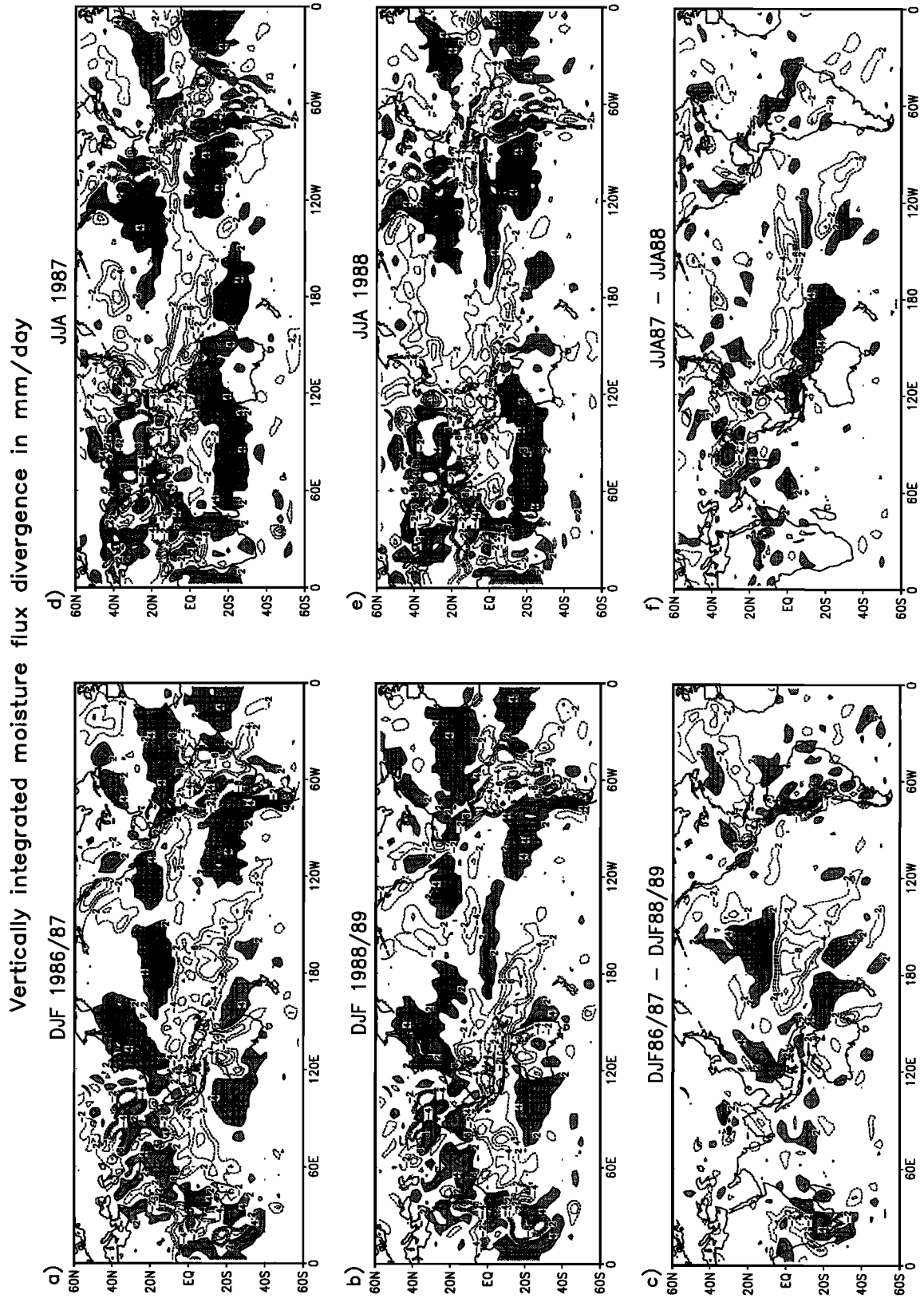

Figure 7. Divergence of vertically integrated moisture flux (mm/d) for (a) DJF 1986/1987, (b) DJF 1988/1989, (c) the difference between them, (d) JJA 1987, (e) JJA 1988, and (f) the difference between them.

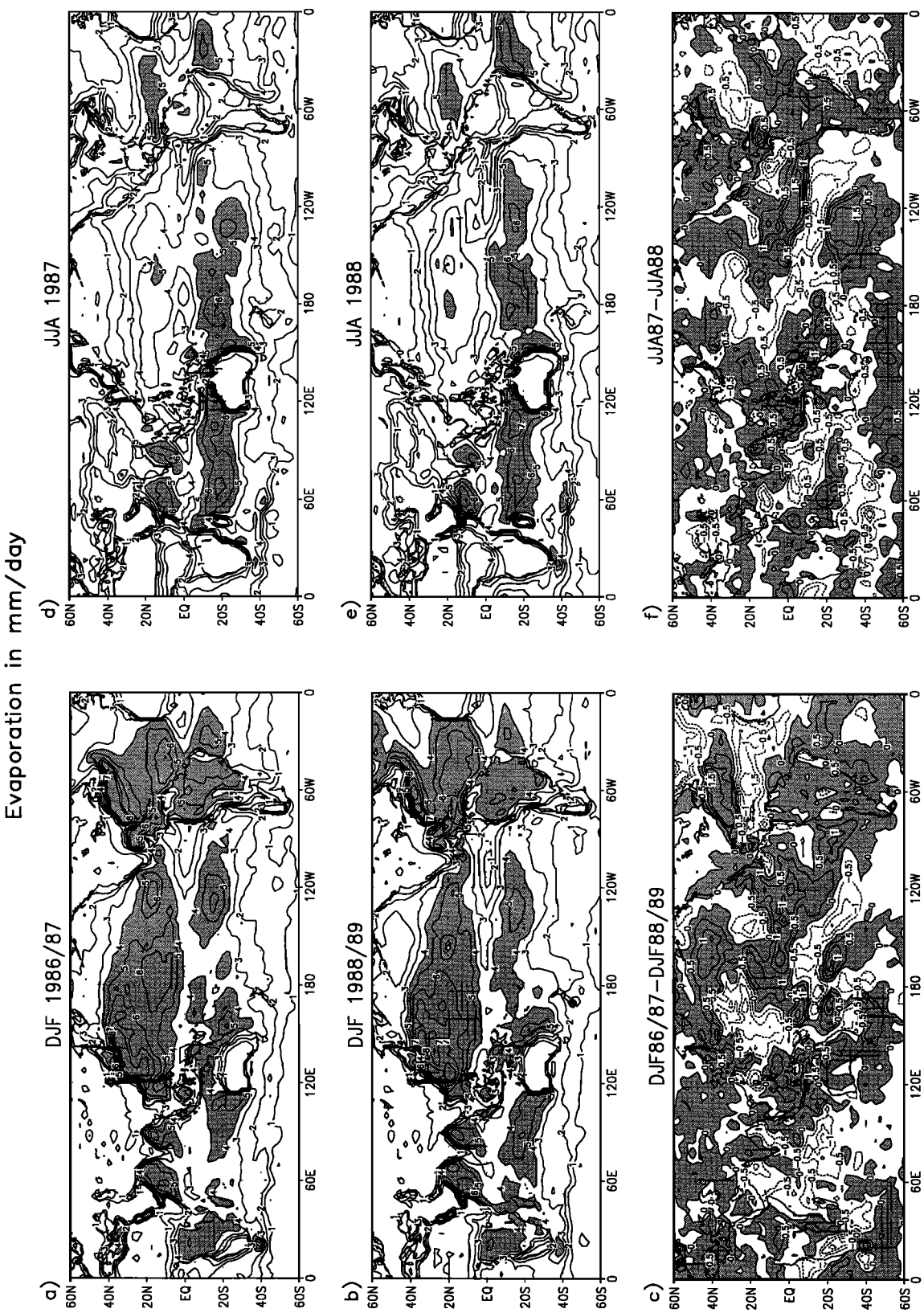

Figure 8. Evaporation (mm/d) for (a) DJF 1986/1987, (b) DJF 1988/1989, (c) the difference between them, (d) JJA 1987, (e) JJA 1988, and (f) the difference between them.

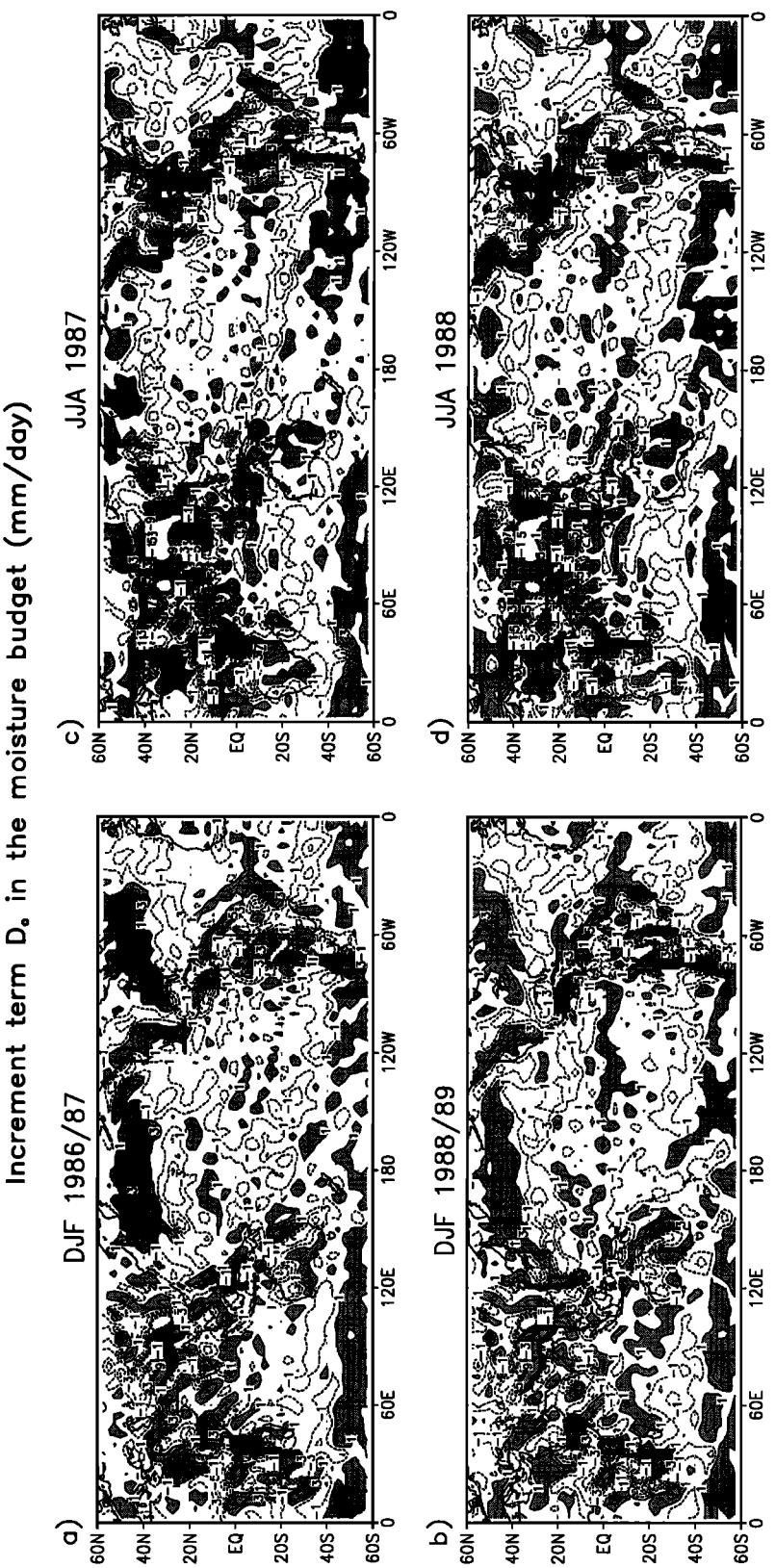

Figure 9. Increment term D_c (mm/d) for (a) DJF 1986/1987, (b) DJF 1988/1989, (c) JJA 1987, and (d) JJA 1988.

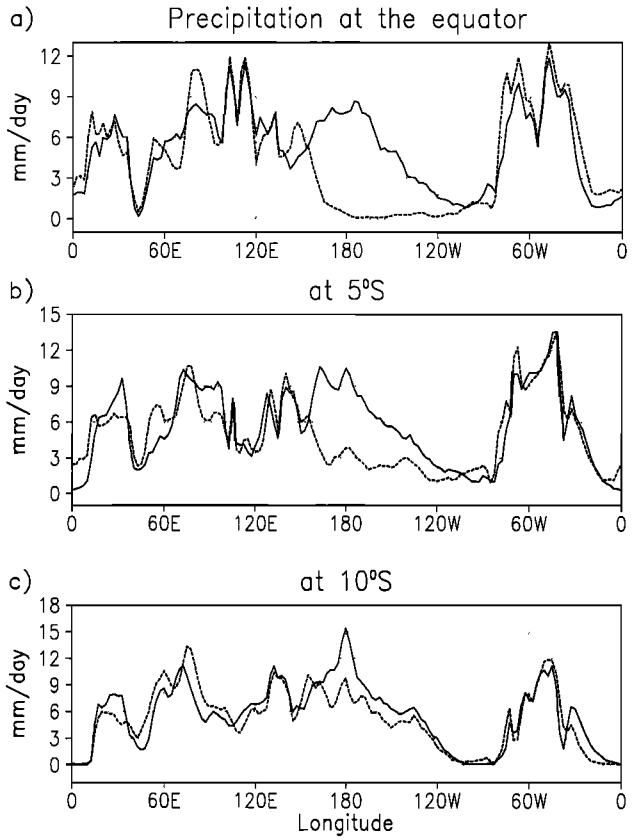

Figure 10. Precipitation in mm/d at (a) the equator, (b) 5°S, and (c) 10°S for DJF 1986/1987 (solid line) and DJF 1988/1989 (dashed line).

with little change over the other parts, and at 10°S the changes are seen only over the Pacific. The rainfall during the El Niño year (DJF 1986/1987) is high over the western Pacific (maxima of around 9 mm/d at 0° and more than 10 mm/d at 5°S (note the difference in the scales). During the La Niña year (DJF 1988/1989), rainfall is much lower. At the equator the largest difference is about 9 mm/d around 180°. These changes indicate ascending motion over the western Pacific and descending motion over the eastern Pacific during the El Niño year. During the La Niña year the ascending motion is reduced even over the western Pacific. Other regions of high rainfall are from around 50°W to 70°W with a drop around 60°W at the equator and 5°S. A careful examination of Figure 1 shows that the rainfall is lower at 60°W with higher values on either side, even in the long-term mean. At a more southern latitude, 10°S, Figure 10 shows only one maximum in this region at 50°W. The high rainfall over the west is associated with the SACZ, and over the east it is associated with the ITCZ. This high rainfall over South America is associated with strong ascending motion, and no major changes are seen between the El Niño and the La Niña years. Another region of high rainfall and so the ascending motion is seen over Indonesia. A region of high rainfall can be seen over central Africa. These regions of high rainfall are separated by low rainfall (descending motion), thus forming cells of rising and sinking motion in the equatorial vertical plane which represents the Walker circulation.

The satellite-measured outgoing longwave radiation (OLR) for the two periods (figures not shown here) shows the large changes from about 150°E to 120°W. In general, regions of high (low) rainfall coincide with low (high) OLR, giving credibility to the precipitation estimation, although OLR shows somewhat higher changes around 60°W and 50°E, particularly at the equator.

Figure 11 shows the precipitable water for the two periods DJF 1986/1987 (solid line) and DJF 1988/1989 (dashed line). The region of large changes in the Pacific noted in Figure 10 at the equator are associated with high precipitable water in DJF 1986/1987 and low precipitable water in DJF 1988/1989. The changes decrease as one moves southward. The sharp change to the west of 60°W in Figure 11 may not be real and may be due to assimilation problems over Andes.

Figures 12 and 13 show, respectively, the divergence of moisture transport and evaporation (both in mm/d) for the two periods DJF 1986/1987 and DJF 1988/1989. As noted earlier, rainfall changes over the western Pacific (Figure 10) are due to changes in the divergence of moisture transport but not due to evaporation. From Figure 13 it can be seen that evaporation in both years decreases (at the equator and 5°S) from about 4 mm/d at 180°W to about 1 mm/d at 120°W. However, from this lowest value the evaporation increases rapidly toward the east, reaching high values (5 mm/d) around 60°W. Thus the high precipitation (around 10 mm/d) in the Amazon region (Figure 10) seems to be accounted partially by the local evaporation (to be precise, evapotranspiration). This agrees with the earlier studies [*Salati and Nobre*, 1991; *Rao et al.*, 1996]. Figure 14 shows D_c values calculated from (5). It can be seen in this figure that D_c values oscillate around zero only at the equator. However, at 5°S and 10°S, D_c values are high in both years in

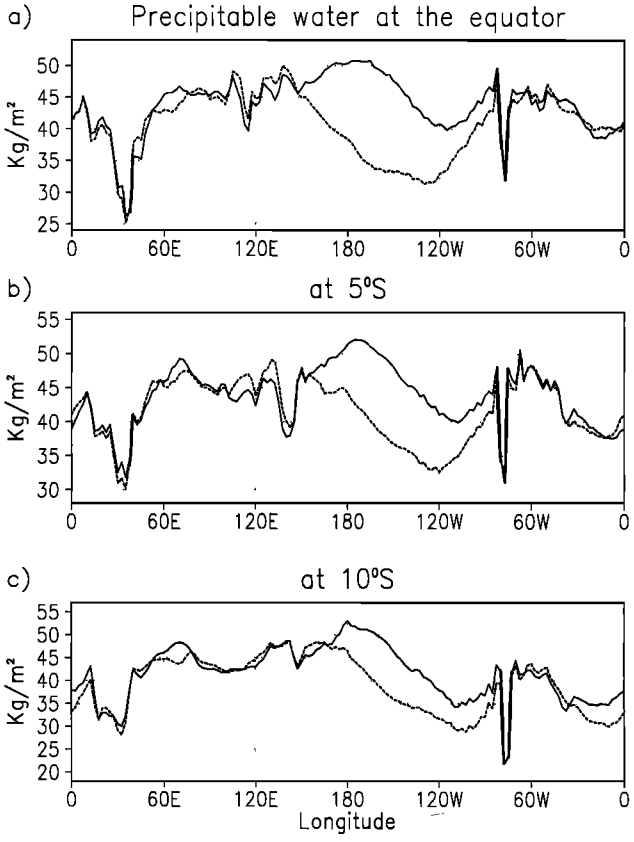

Figure 11. Precipitable water in kg/m^2 (mm) at (a) the equator, (b) 5°S, and (c) 10°S for DJF 1986/1987 (solid line) and DJF 1988/1989 (dashed line).

the regions of highlands and east coasts. These large values seem to stem from the errors in the calculation of moisture flux divergence over Pacific from about 150°E to 90°W. D_c values are low at 0°S and 5°S, showing that some conclusions regarding the moisture budget can be drawn confidently.

As can be seen in Figure 10, precipitation is very low (almost zero at the equator) between 180° and 120°W during the La Niña year, DJF 1988/1989. In this region there is divergence (Figure 12) during this period. Thus evaporation is almost totally used in the divergence of moisture flux. During the El Niño year, DJF 1986/1987, convergence of the moisture flux is noted, and the high precipitation (around 8 mm/d at 180°) is accounted to a large extent by this moisture flux convergence (5 mm/d around 180°). This shows the important role of moisture flux convergence for the interannual variation of rainfall in this region. *Cornejo-Garrido and Stone* [1977] indirectly inferred the role of moisture flux convergence for the precipitation in this region from the heat balance. However, the present study not only shows the importance of moisture flux convergence for the precipitation over the western Pacific by an actual calculation of moisture budget but also notes the large interannual differences (divergence in DJF 1988/1989 and convergence in DJF 1986/1987).

The moisture budget is evaluated for JJA 1987 and JJA 1988 also. For the sake of brevity we will not show the figures here. The general features, particularly the differences between the El Niño (JJA 1987) and the La Niña (JJA 1988) years are very similar to those noted for the DJF. Again, D_c values are around zero in the western Pacific. In this region the differences in rainfall between El Niño and La Niña years are accounted mainly by changes in moisture flux divergence. The rainfall over the Amazon region is very much suppressed in JJA 1987 and JJA 1988.

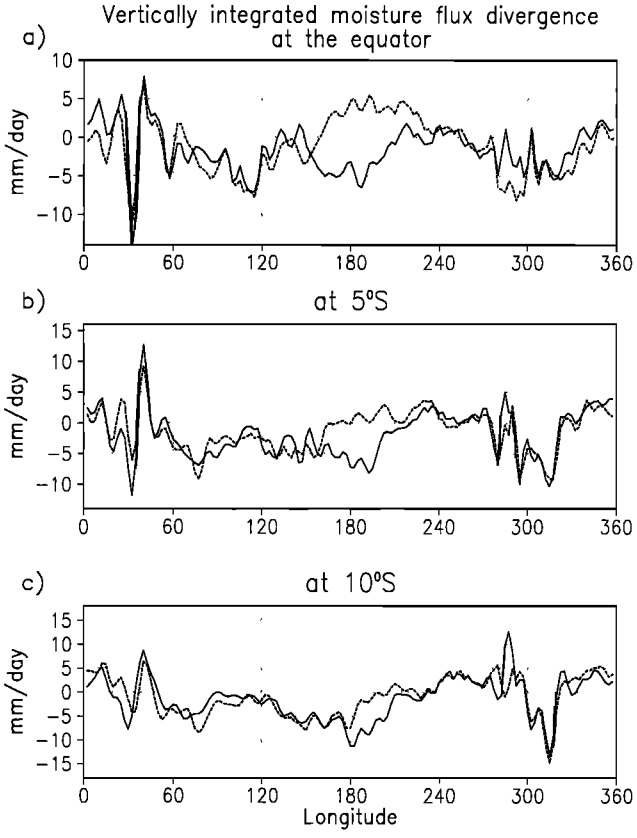

Figure 12. Vertically integrated moisture flux divergence in mm/d at (a) the equator, (b) 5°S, and (c) 10°S for DJF 1986/1987 (solid line) and DJF 1988/1989 (dashed line).

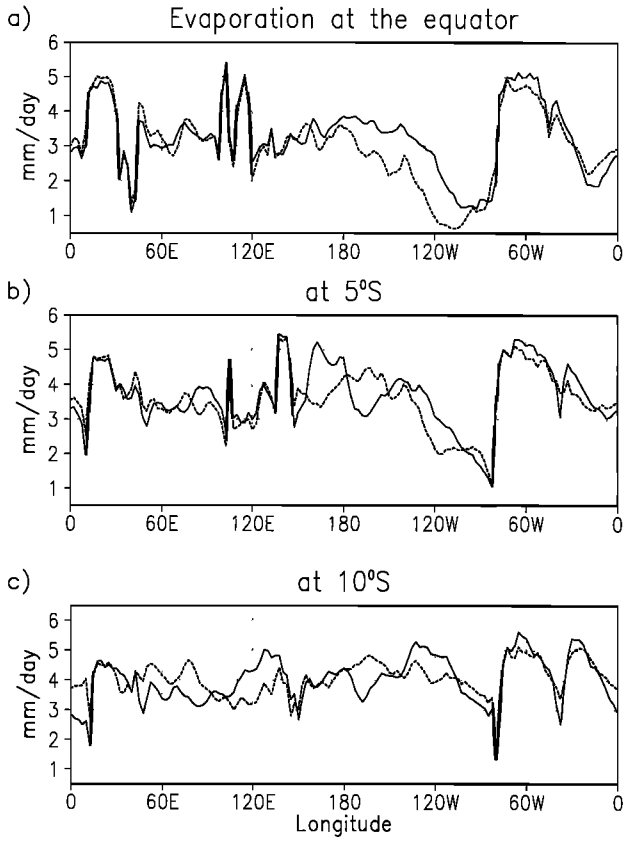

Figure 13. Evaporation in mm/d at (a) the equator, (b) 5°S, and (c) 10°S for DJF 1986/1987 (solid line) and DJF 1988/1989 (dashed line).

6. Concluding Remarks

In an earlier study, *Mo and Higgins* [1996] concluded that the interannual variations in the moisture budget associated with the 1986–1989 ENSO cycle are captured by the NCEP reanalysis data. However, in their article there was only a brief discussion of this ENSO event. In the present study a detailed discussion of the moisture budget is given, using the same data. Also, the moisture budget of the Walker circulation is studied. Some of the principle conclusions are given below.

Comparison of the (13 years) mean rainfall and evaporation characteristics of the NCEP reanalysis for January, April, July, and October with other independent data showed that the general precipitation zones associated with the ITCZ, SPCZ, and SACZ are captured by this analysis. However, the seasonal variations are not reproduced well. There seems to be some problem in the NCEP reanalysis in the reproduction of the ITCZ in the eastern Pacific. The overall characteristics of latent heat flux (evaporation) in the NCEP reanalysis seems to be in qualitative agreement with other independent data.

A comparison of rainfall data for the 1986–1989 ENSO cycle with *Huffman et al.* [1997] showed that the NCEP reanalysis reproduced the rainfall patterns over the tropics. The NCEP reanalysis seems to capture the general characteristics of the

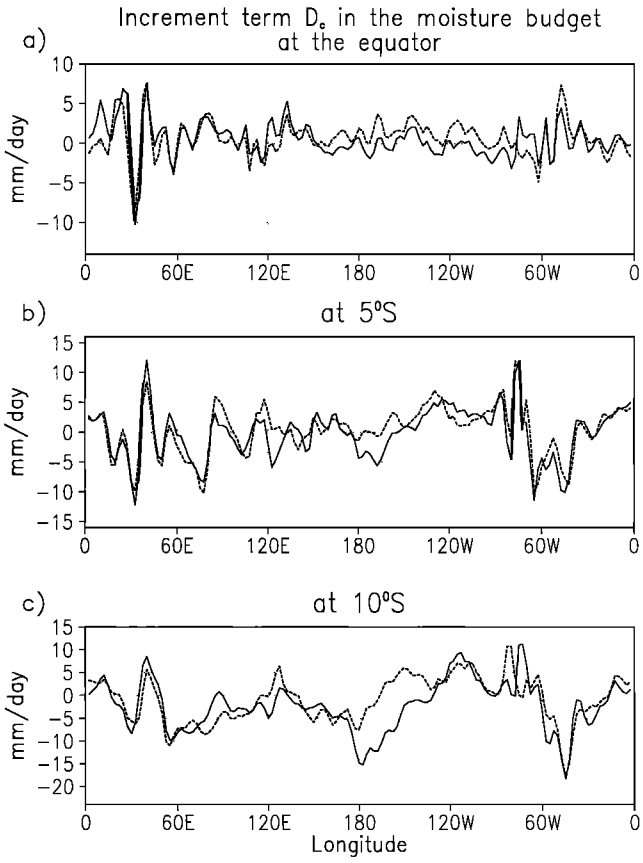

Figure 14. Increment term D_c (mm/d) at (a) the equator, (b) 5°S, and (c) 10°S for DJF 1986/1987 (solid line) and DJF 1988/1989 (dashed line).

vertically integrated moisture transport in the tropics, such as the cross-equatorial moisture transport over the Indian Ocean with high values near the Somali coast in JJA. Over the western Pacific the differences between the two periods (El Niño and La Niña) are associated with the differences in moisture convergence but not evaporation. The increment term (D_c) shows large values over the mountaineous regions.

Some of the new results of the present study are regarding the moisture budget of the Walker circulation. The results showed that the large differences in rainfall between the two contrasting years (El Niño and La Niña) in the western Pacific are accounted by the differences in moisture flux convergence. This shows the important role of moisture convergence in this region as inferred indirectly by *Cornejo-Garrido and Stone* [1977]. However, over the Amazon region, evapotranspiration seems to have an important role in the local precipitation.

References

Ba, M. B., R. Frouin, and S. E. Nicholson, Satellite-derived interannual variability of West African rainfall during 1983–88, *J. Appl. Meteorol.*, *34*, 411–431, 1995.

Bjerknes, J., Atmospheric teleconnections from the equatorial Pacific, *Mon. Weather Rev.*, *97*, 163–172, 1969.

Businger, J. A., Interactions of sea and atmosphere, *Rev. Geophys.*, *13*, 720–822, 1975.

Cayan, D. R., Variability of latent and sensible heat fluxes estimated using bulk formulae, *Atmos. Ocean*, *30*, 1–42, 1992.

Chen, T. C., Global water vapor flux and maintenance during FGGE, *Mon. Weather Rev.*, *113*, 1801–1819, 1985.

Chen, T. C., and H. Van Loon, Interannual variation of the tropical easterly jet, *Mon. Weather Rev.*, *115*, 1739–1759, 1987.

Cornejo-Garrido, A. G., and P. H. Stone, On the heat balance of the Walker circulation, *J. Atmos. Sci.*, *34*, 1155–1162, 1977.

Da Silva, A. M., C. C. Young, and S. Levitus, Atlas of surface marine data 1994, in *Algorithms and Procedures*, vol. 1, *NOAA Atlas NESDIS 6*, U.S. Dep. of Commer., Natl. Oceanic and Atmos. Admin., NESDIS, Washington, D. C., 1994.

Deser, C., and J. M. Wallace, Large-scale atmospheric circulation features of warm and cold episodes in the tropical Pacific, *J. Clim.*, *3*, 1254–1281, 1990.

Glantz, M., R. Katz, and N. Nicholls, *Teleconnections Linkng Worldwide Climate Anomalies*, 535 pp., Cambridge Univ. Press, New York, 1991.

Hsiung, J., Mean surface energy fluxes over the global oceans, *J. Geophys. Res.*, *91*, 10,585–10,606, 1986.

Huffman, G. J., R. F. Adler, P. Arkin, A. Chang, R. Ferrao, A. Gruber, J. Janowiak, A. Menab, B. Rudolf, and U. Schneider, The Global Precipitation Climatology Project (GPCP) combined precipitation data set, *Bull. Am. Meteorol. Soc.*, *78*, 5–20, 1997.

Jourdan, D., and C. Gautier, Comparison between global latent heat flux computed from multisensor (SSM/I and AVHRR) and from in situ data, *J. Atmos. Oceanic Technol.*, *12*, 46–71, 1995.

Kalnay, E., and coauthors, The NCEP/NCAR 40 year reanalysis project, *Bull. Am. Meteorol. Soc.*, *77*, 437–471, 1996.

Krishnamurti, T. N., H. S. Bedi, and M. Subramaniam, The summer monsoon of 1987, *J. Clim.*, *2*, 321–340, 1989.

Krishnamurti, T. N., H. S. Bedi, and M. Subramaniam, The summer monsoon of 1988, *Meteorol. Atmos. Phys.*, *42*, 19–37, 1990.

Liu, W. T., K. B. Katsaros, and J. A. Businger, Bulk parameterization of air-sea exchanges of heat and water vapor including molecular constrains at the interface, *J. Atmos. Sci.*, *36*, 1722–1735, 1979.

Mo, K. C., and R. W. Higgins, Large-scale atmospheric moisture transport as evaluated in NCEP/NCAR and NASA/DAO reanalysis, *J. Clim.*, *9*, 1531–1545, 1996.

Murakami, T., T. Nakazawa, and J. He, On the 40–50 day oscillation during the 1979 northern hemisphere summer, II, Heat and moisture budget, *J. Meteorol. Soc. Jpn.*, *62*, 469–484, 1984.

Newell, J. E., J. W. Kidson, D. G. Vincent, and G. J. Boer, *The General Circulation of the Tropical Atmosphere*, vol. 2, 371 pp., MIT Press, Cambridge, Mass., 1974.

Oberhuber, J. M., An atlas based on the "COADS" data set: The budget of heat, buoyancy and turbulent kinetic energy at the surface of the global ocean, *Rep. 15*, 28 pp., Max Plank Inst. for Meteorol., Hanover, Germany, 1988.

Ramage, C. S., and A. M. Hori, Meteorological aspects of El Niño, *Mon. Weather Rev.*, *109*, 1827–1835, 1981.

Rao, V. B., and M. C. Lima, The summer circulations during two contrasting years, in 20th Annual Climate Diagnostics Workshop, Seattle, Wash., 1995.

Rao, V. B., and V. S. Marques, Water vapor characteristics over northeast Brazil during two contrasting years, *J. Clim. Appl. Meteorol.*, *22*, 440–444, 1984.

Rao, V. B., I. F. A. Cavalcanti, and K. Hada, Annual variation of rainfall over Brazil and water vapor characteristics over South America, *J. Geophys. Res.*, *101*, 26,539–26,551, 1996.

Rasmusson, E., and K. C. Mo, Large-scale atmospheric water vapor transport as evaluated from NCEP global analysis and forecast products, *J. Clim.*, *9*, 3276–3297, 1996.

Rosen, R. D., and D. A. Salstein, A comparison between circulation statistics computed from observational data and NMC Hough analysis, *Mon. Weather Rev.*, *108*, 1226–1247, 1980.

Rowell, D. P., C. P. Folland, K. Maskel, and M. N. Ward, Variability of summer rainfall over tropical north Africa (1906–92): Observations and modelling, *Q. J. R. Meteorol. Soc.*, *121*, 669–704, 1995.

Salati, E., and C. A. Nobre, Possible climate impacts of tropical deforestation, *Clim. Change*, *19*, 177–196, 1991.

Schemm, J. K., S. Schubert, J. Terry, and S. Bloom, Estimates of monthly mean soil moisture for 1979–89, *NASA Tech. Memo. 104571*, 252 pp., 1992.

Schubert, S. D., C. K. Park, R. B. Rood, C. Y. Wu, R. W. Higgins, Y. Kondratyeva, A. Molod, and T. Takacs, A multiyear assimilation with the GOES-1 system: An overview and results, *NASA Tech. Memo. 104604*, 183 pp., 1995.

Smith, S. D., Coefficients for sea surface wind stress, heat flux and wind

profiles as a function of wind speed and temperature, *J. Geophys. Res.*, *93*, 15,467–15,472, 1988.

Trenberth, K. E., Climate diagnostics from global analysis: Conservation of mass in ECMWF analysis, *J. Clim.*, *4*, 707–722, 1991.

Trenberth, K. E., and C. J. Guillemot, Evaluation of atmospheric moisture budget as seen from analysis, *J. Clim.*, *8*, 2255–2272, 1995.

Trenberth, K. E., and C. J. Guillemot, Physical process involved in the 1988 drought and 1993 floods in North America, *J. Clim.*, *9*, 1288–1298, 1996.

Vincent, D. C., The South Pacific Convergence Zone (SPCZ): A review, *Mon. Weather Rev.*, *122*, 1949–1970, 1994.

World Climate Research Program (WCRP), *Proceedings of the WCRP Workshop on Air-Sea Flux Fields for Forcing Ocean Models and Validating GCMs*, Eur. Cent. for Medium-Range Weather Forecasts, Reading, England, 1996.

I. F. A. Cavalcanti, S. R. Chapa, and V. Brahmananda Rao, Instituto Nacional de Pesquisas Espaciais (INPE), São José dos Campos, São Paulo, 12201-970, Brazil.

(Received July 7, 1997; revised January 7, 1998;
accepted March 9, 1998.)